Relativistic two-fluid model of nucleus-nucleus collisions*

Anthony A. Amsden, Alfred S. Goldhaber,† Francis H. Harlow, and J. Rayford Nix
Theoretical Division, Los Alamos Scientific Laboratory, University of California, Los Alamos, New Mexico 87545
(Received 22 November 1977)

To take into account the expected partial transparency of nuclei during collisions at high energy, we introduce a two-fluid dynamical model, in which coupled relativistic equations of motion are solved for separate target and projectile nuclear fluids. The terms in the equations that couple the two nuclear fluids are obtained from the cross section and momentum transfer for individual nucleon-nucleon collisions. At low relative velocities the target and projectile fluids merge, in which case the conventional one-fluid dynamical model is recovered. For a given nuclear equation of state and for given initial conditions, the equations of motion are solved as functions of time for the nucleon number density, momentum density, energy density, pressure, and velocity for each fluid. This is done in three spatial dimensions by means of a relativistic generalization of a standard particle-in-cell finite-difference computing method for multiphase fluid-dynamics problems. For each of several impact parameters, the velocity distribution at some large time is converted to an energy and angular distribution for the expanding matter. Integration of these results over impact parameter then gives the double differential cross section $d^2\sigma/dEd\Omega$. For $^{20}Ne + ^{238}U$ at laboratory bombarding energies per nucleon of 250 MeV, 400 MeV, and 2.1 GeV, as well as for $^4He + ^{238}U$ at a laboratory bombarding energy per nucleon of 400 MeV, we compare calculated and experimental energy spectra for outgoing charged particles at several laboratory angles. The calculations reproduce correctly the experimental slopes at each angle, as well as the overall decrease in the experimental cross section when going from forward to backward angles. However, for $^{20}Ne + ^{238}U$ at laboratory bombarding energies per nucleon of 250 and 400 MeV, the calculated values at 30° are only one-third the experimental values. Also, for $^4He + ^{238}U$ at a laboratory bombarding energy per nucleon of 400 MeV, the calculated values at all angles are substantially smaller than the experimental values. As a prediction for future experiments, we also use the theory in a context where our numerical approximations and simplifications (such as neglecting the diffuseness of the nuclear surface) should be more reliable, to deduce results for $^{238}U + ^{238}U$ at laboratory bombarding energies per nucleon of 250 MeV and 2.1 GeV. By means of a one-dimensional calculation we also study the maximum compression and excitation that can be achieved in such collisions. The maximum rest-frame compression is about 2.4 to 2.6 at a bombarding energy per nucleon of 250 MeV, and is about 6 to 8 at a bombarding energy per nucleon of 2.1 GeV. The available energy is primarily in the form of compressional energy, with little in the form of internal excitation energy. Significant rest-frame compressions (greater than twice normal density for 250 MeV and greater than 3 times normal density for 2.1 GeV) are achieved for substantial numbers of nucleons and substantial time periods.

[NUCLEAR REACTIONS $^{20}Ne + ^{238}U$, $E_{bom}/20 = 250$ MeV, 400 MeV, 2.1 GeV; $^4He + ^{238}U$, $E_{bom}/4 = 400$ MeV; $^{238}U + ^{238}U$, $E_{bom}/238 = 250$ MeV, 2.1 GeV. Calculated $d^2\sigma/dEd\Omega$ for outgoing charged particles. Relativistic two-fluid dynamical model, nuclear equation of state, nuclear matter at high density and high excitation energy.]

I. INTRODUCTION

The description of a nucleus as a fluid drop has been a useful tool almost from the beginning of nuclear theory. It is natural then to study nuclear collisions with the techniques of fluid dynamics. As in any such phenomenological approach, the goal is to describe the response of a system that contains many degrees of freedom by means of a model which contains a few parameters whose values are determined from comparisons with experimental results. In the case of nuclei, the parameters are interpreted in terms of macroscopic or bulk properties of nuclear matter, expecially its equation of state.

Several attempts have already been made to describe nucleus-nucleus collisions by means of a conventional hydrodynamical model,[1-15] which we refer to as a one-fluid model. In this model both the target and projectile nuclei are treated as drops of nuclear fluid which evolve according to the laws of standard hydrodynamics. The adjustable parameters in the model are associated primarily with the nuclear equation of state, which may be regarded as the unknown quantity to be determined from comparisons with experimental data.

An essential assumption in the one-fluid model is that when two bits of nuclear fluid overlap, they share their momentum and energy instantaneously, coming to equilibrium as a single bit of fluid at rest in the center-of-momentum frame of the

two bits. While this assumption simplifies the model, it is in contradiction with experimental information from nucleon-nucleon collisions[16] and even nucleon-nucleus collisions.[17-19] These experiments suggest that at high energies, a projectile deposits only a limited fraction of its energy and momentum in a target. If this same principle applies also to collisions of two bits of nuclear matter, then the instantaneous equilibration assumed in the one-fluid model is incorrect for large relative velocities.

In an attempt to take into account these results from elementary-particle physics, we have constructed a relativistic two-fluid model of nuclear collisions, in which coupled fluid dynamical equations are solved for separate target and projectile nuclear fluids. The model is designed so that at high relative velocities the projectile fluid deposits only a limited fraction of its energy and momentum in the target fluid, and vice versa, whereas at low relative velocities the target and projectile fluids merge, in which case the conventional one-fluid model is recovered.

We describe in Sec. II this two-fluid model, along with the techniques that are used to solve it. Some calculated results and comparisons with experimental data are presented in Sec. III, and our conclusions are given in Sec. IV.

II. TWO-FLUID MODEL

The equations of motion for the target and projectile nuclear fluids express the conservation of nucleon number, energy, and momentum, plus the transfer of energy and momentum between the two fluids. For a given fluid, the relativistic equations of motion are analogous to those for the conventional one-fluid dynamical model,[13,14,20] but contain, in addition, coupling terms that describe the transfer of energy and momentum from one fluid to the other when they collide. As before, we neglect the surface energy, Coulomb energy, nuclear viscosity, thermal conductivity, and single-particle effects, as well as the production of additional particles and the associated radiative loss of energy from the system.

A. High relative velocities

When the relative velocity of the two fluids is large compared to the Fermi velocities of the nucleons comprising each fluid, the relativistic equations of motion for fluid 1 are written as

$$\partial N_1/\partial t + \nabla\cdot(\vec{v}_1 N_1) = 0\,, \tag{1}$$

$$\partial \vec{M}_1/\partial t + \nabla\cdot(\vec{v}_1\vec{M}_1) = -\nabla p_1 - D_c(\gamma_1\vec{v}_1 - \gamma_2\vec{v}_2) - D_r\gamma_1\vec{v}_1\,, \tag{2}$$

and

$$\partial E_1/\partial t + \nabla\cdot(\vec{v}_1 E_1) = -\nabla\cdot(\vec{v}_1 p_1) - D_c(\gamma_1 - \gamma_2) - D_r\gamma_1\,; \tag{3}$$

those for fluid 2 are obtained by interchanging the subscripts 1 and 2. Here N_i, $\vec{M}_i$, E_i, and $\vec{v}_i$ are the nucleon number density, momentum density, energy density, and flow velocity, respectively, of fluid i in the calculational frame (which we take to be the laboratory frame), and p_i is the pressure of fluid i in its rest frame. The computational-frame quantities are related to rest-frame quantities by[13,14,20]

$$N_i = \gamma_i n_i\,, \tag{4}$$

$$\vec{M}_i = \gamma_i^{\,2}(\epsilon_i + p_i)\vec{v}_i\,, \tag{5}$$

and

$$E_i = \gamma_i^{\,2}(\epsilon_i + p_i) - p_i\,, \tag{6}$$

where n_i and ϵ_i are, respectively, the nucleon number density and energy density of fluid i in its rest frame and $\gamma_i = (1 - v_i^{\,2})^{-1/2}$, with velocities measured here and throughout the paper in units of the speed of light. The pressure p_i of fluid i is related to n_i and ϵ_i through the nuclear equation of state, which is discussed in Sec. II C.

The coupling terms are derived by considering the energy and momentum transferred to a free target nucleon at rest when it is struck by a free projectile nucleon, and then Lorentz transforming the results to an arbitrary computational reference frame. These coupling terms are resolved into parts that correspond to the *conservation* of total energy and momentum for the two-fluid system and parts that correspond to the *radiation* of energy and momentum away from the system. The former involve the conservative drag function

$$D_c = N_1 N_2 v_{\rm rel}\sigma K/Y\,, \tag{7}$$

and the latter involve the radiative drag function

$$D_r = N_1 N_2 v_{\rm rel}\sigma[K/(Y+1) - K'/Y]X^2/Y\,, \tag{8}$$

where[21]

$$v_{\rm rel} = [(\vec{v}_1 - \vec{v}_2)^2 - (\vec{v}_1\times\vec{v}_2)^2]^{1/2}\,. \tag{9}$$

In the nonrelativistic limit, $v_{\rm rel}$ is the magnitude of the relative velocity of the two fluids. However, for relativistic velocities $v_{\rm rel}$ no longer has this interpretation.

In Eqs. (7) and (8), the product $N_1 N_2 v_{\rm rel}$ gives the Lorentz-invariant Møller flux factor for two-body collisions,[21] and σ is the total cross section at the given relative velocity. The quantity K is defined so that $K\vec{v}$ is the mean longitudinal momentum transferred to a nucleon at rest by an

incident nucleon of velocity $\vec{v}$, while $K'v^2$ is the mean energy transferred to the struck nucleon. Clearly, a two-nucleon collision imparts transverse momentum to the struck nucleon. Averaged over many collisions, this transverse momentum vanishes, but the associated transverse kinetic energy is included in the mean energy transfer $K'v^2$. The quantities X and Y are defined by

$$X = \gamma_1\gamma_2 v_{\text{rel}} \tag{10}$$

and

$$Y = (X^2 + 1)^{1/2} . \tag{11}$$

In the rest frame of one fluid, the invariant quantity X is simply the momentum divided by the mass of a nucleon moving with the other fluid.

In order that there be net energy loss rather than net energy gain, the radiative drag function D_r must be positive, which means that K and K' must satisfy the inequality

$$K'(X) \leq K(X)Y/(Y+1) . \tag{12}$$

For two-nucleon collisions, K' has also a lower bound because the lowest-mass state with quantum numbers of a baryon is a nucleon, namely

$$K'X^2/Y^2 + m_0 \geq (K^2X^2/Y^2 + m_0^2)^{1/2} , \tag{13}$$

where m_0 is the nucleon rest mass. The specific choices used for K and K', as well as σ, are discussed in Sec. II D.

The above drag terms describe friction between the two fluids entirely in terms of two-body collisions between nucleons moving with the velocity of fluid 1 and nucleons moving with the velocity of fluid 2. This is reasonable only if the relative velocity of the two fluids is large compared to the Fermi velocities of the nucleons comprising each fluid. By neglecting the Fermi velocities, we are underestimating the collision rate between fluid-1 nucleons and fluid-2 nucleons, and hence, the strength of the coupling between the two fluids. In addition, the above formulation assumes that the friction is independent of the degree of excitation of either fluid, i.e., that excited nucleons have the same cross section and accept the same energy and longitudinal momentum as ordinary nucleons when struck by other nucleons. This assumption is made primarily to avoid introducing unnecessary adjustable parameters into the theory, but at least for very-high-energy collisions ($\gtrsim$15 GeV) it is supported by experimental data on the production of 1.4 GeV N^*'s in proton-nucleus collisions.[22] A possible later refinement would be to permit the product σK to vary with the internal energy of the fluids.

B. Intermediate and low relative velocities

When the relative velocity of the two fluids is less than the Fermi velocities of the nucleons comprising each fluid, the target and projectile fluids merge, and the conventional one-fluid dynamical model is recovered. We accomplish this transition by using an averaging procedure during the early stages of each time step. As discussed more fully in Sec. II E, these early stages consist of integrating modified versions of Eqs. (1)–(3) forward in time. The modified versions include only the explicit $\partial/\partial t$ terms and the drag terms. Whenever the relative-velocity variable X of Eq. (10) is less than an upper critical value X_u, we perform these early-stage integrations in two different ways; then we use a weighted average of the two different results as input for later calculational stages of the time step.

In the first way of performing the early-stage integrations, we use the two-fluid formulation but multiply each of the drag functions D_c and D_r by $\alpha(X)$, where $\alpha(X)$ varies continuously through intermediate velocities from $\alpha = 1$ at $X = X_u$ to $\alpha = 0$ at $X = X_1$, with X_1 the lower critical value at which the two fluids merge into one fluid. Therefore, when the two fluids merge, the explicit drag of one component on the other disappears. This first stage of integration leads to intemediate values p_i and $\vec{v}_i$ for the two fluids considered separately.

In the second way of performing the early-stage integration, we define the total-fluid quantities

$$N = N_1 + N_2 , \tag{14}$$

$$\vec{M} = \vec{M}_1 + \vec{M}_2 , \tag{15}$$

and

$$E = E_1 + E_2 . \tag{16}$$

The quantities p and $\vec{v}$ for the total fluid are then determined by solving the early-stage relativistic equations of motion for the one-fluid dynamical model.[14] For the next stages of the time step [where we take into account the previously ignored terms of Eqs. (1)–(3)], the pressure and velocity of the ith fluid are taken to be

$$\langle p_i \rangle = \alpha p_i + (1-\alpha)N_i p/N \tag{17}$$

and

$$\langle \vec{v}_i \rangle = \alpha \vec{v}_i + (1-\alpha)\vec{v} . \tag{18}$$

In other words, the models that apply at high relative velocities and at low relative velocities are simply interpolated smoothly at intermediate velocities.

C. Nuclear equation of state

In order to study the effects of the two-fluid assumptions, we have begun by keeping fixed all other quantities in the previous one-fluid calculations,[14,15] including in particular the nuclear equation of state. This equation of state is obtained from the effective two-nucleon interaction that consists of an attractive Yukawa function multiplied by a quadratic momentum-dependent term.[23] This leads to a rest-frame energy per nucleon ϵ/n of the form

$$\frac{\epsilon}{n} = m_0 + a\left(\frac{n}{n_0}\right)^{2/3} - b\frac{n}{n_0} + c\left(\frac{n}{n_0}\right)^{5/3} + \frac{I}{n}, \tag{19}$$

where m_0 is the nucleon rest mass, $n_0 = 3/4\pi r_0^3$ is the equilibrium value of n, and I/n is the rest-frame internal excitation energy per nucleon. In this equation and below, the various quantities that appear refer either to the combined nuclear fluid for the entire system, or to fluid 1 or fluid 2 separately.

For the specific choices[23] of 1.2049 fm for r_0 and -15.677 MeV for the nonrelativistic energy per nucleon at equilibrium (excluding rest energy), the values of the three constants that appear in Eq. (19) are $a = 19.88$ MeV, $b = 69.02$ MeV, and $c = 33.46$ MeV. The resulting value of the nuclear compressibility coefficient $9n_0^2\partial^2(\epsilon/n)/\partial n^2|_0$ is 294.8 MeV. These particular constants refer to symmetric nuclear matter with zero Coulomb interaction. If account were taken of the neutron excess and Coulomb interaction present in heavy-ion collisions, then the compressibility coefficient would be reduced slightly.

The pressure p is obtained from the relationship $p = n^2\partial(\epsilon/n)/\partial n|_S$, with differentiation at constant entropy S. The relationship between I/n and the nuclear temperature is taken from a nonrelativistic Fermi-gas model for the thermal motion of the nucleons relative to the hydrodynamic flow, for which $n^2\partial(I/n)/\partial n|_S = \frac{2}{3}I$. This is the exact result for a nonrelativistic Fermi-gas model, instead of being true only to second order in the nuclear temperature, as is often implied. Finally, the pressure is given by

$$\begin{aligned} p &= [\tfrac{2}{3}a(n/n_0)^{5/3} - b(n/n_0)^2 + \tfrac{5}{3}c(n/n_0)^{8/3}]n_0 + \tfrac{2}{3}I \\ &= [-\tfrac{2}{3}m_0(n/n_0) - \tfrac{1}{3}b(n/n_0)^2 + c(n/n_0)^{8/3}]n_0 + \tfrac{2}{3}\epsilon\,. \end{aligned} \tag{20}$$

Because of the $(n/n_0)^{5/3}$ term in Eq. (19), our expression for the energy per nucleon leads to a sound velocity $v_s = (\partial p/\partial\epsilon|_S)^{1/2}$ that exceeds the speed of light for $n/n_0 > 5.32$, if the internal excitation energy is zero. This is of course physically impossible, which means that within a fluid-dynamics description, the true energy per nucleon at very high densities increases less rapidly with increasing n/n_0 than does that given by Eq. (19). In fact, the requirement that the sound velocity not exceed the speed of light means that for very high densities the energy per nucleon can increase no faster than n/n_0 to the first power.

In a heavy-ion collision the pressure is positive during the initial compression stage and negative during the later expansion stage, at which time the driving forces attempt to form the matter into small clusters of near-equilibrium density. These clusters would be physically meaningful if properly calculated, but we are unable to do this in our model because we are neglecting the surface energy, Coulomb energy, and single-particle corrections, and because the finite-difference solution of the equations does not resolve them. Nevertheless, we know that in the true situation these particles will cluster to zero pressure, and we accordingly set the pressure to zero when it would otherwise be negative.

D. Choice of coupling functions

In the calculations reported here we use the energy-conserving form for the coupling terms, in which the radiative drag coefficient D_r is zero. If we set

$$K'(X) = [1 - \omega(X)]\,K(X)\,Y/(Y+1)\,, \tag{21}$$

then energy conservation is equivalent to using the maximum value of K' allowed by Eq. (12), namely the value with $\omega(X) = 0$. The use of this energy-conserving form corresponds to the instantaneous reabsorption of any particles that are produced during the collision process. This means that those degrees of freedom associated with particle production are taken into account only implicitly through the nuclear equation of state, which accordingly should be softened to yield a lower pressure than that obtained with purely nucleonic degrees of freedom. When there is radiation of energy and momentum from the system, $\omega(X)$ is greater than zero. An upper bound on $\omega(X)$, determined from Eq. (13), is

$$\omega(X) \leq 1 - K(Y+1)/[(K^2X^2 + m_0^2Y^2)^{1/2} + m_0Y]\,. \tag{22}$$

We determine the function $K(X)$ by considering the mean longitudinal momentum transfer per collision in the limits of low and high relative velocities and by interpolating smoothly at intermediate relative velocities. For isotropic elastic scattering of indistinguishable nucleons at nonrelativistic velocities, the mean longitudinal momentum transfer is one-fourth the incident

momentum, which means that $K(X) \to \frac{1}{4}m_0$ as $X \to 0$. At first thought, one might have expected that $K(X) \to \frac{1}{2}m_0$ as $X \to 0$. However, if the incident projectile nucleon loses more than one-half its momentum, it is naturally identified as the outgoing *target* nucleon. Therefore, the meaningful range of longitudinal momentum transfer is only from zero to one-half the incident momentum. Because the momentum transfer is linear in the cosine of the center-of-mass scattering angle, its average value is simply the middle of its range.

At the other extreme of high relative velocities, the target nucleon is excited during the collision from its ground state with energy m_0 to an excited state with energy m^* and transverse momemtum q_T. This produces a longitudinal momentum transfer of $\frac{1}{2}(m^{*2}+q_T{}^2-m_0{}^2)/m_0$, independent of projectile excitation. For an excited state whose energy is $m^*=\sqrt{2}m_0$ (a typical value), neglecting the small effect of transverse momentum, one finds that $K(X) \to \frac{1}{2}m_0$ as $X \to \infty$. To reproduce these two limits, as well as the threshold for pion production at $X \approx 1$, we choose

$$K(X)=\tfrac{1}{2}m_0\left(1-\frac{1}{2(X^2+1)}\right). \tag{23}$$

This function reproduces the mean experimental longitudinal momentum transfer per collision for free nucleon-nucleon scattering at all relative velocities[16] with an accuracy of about 20%. To verify this at intermediate velocities, it is necessary to take into account the more complicated kinematics of finite projectile energy, which make the longitudinal momentum of the struck target sensitive to projectile excitation and transverse momentum transfer, as well as to target excitation. These relevant quantities may be inferred from the tables in Ref. 16.

For the interpolating function $\alpha(X)$ that determines the transition from two separate fluids at high relative velocities to a single fluid at low relative velocities, we use at this stage the first-degree spline function

$$\alpha(X)=\begin{cases} 0, & X \le X_l, \\ (X-X_l)/(X_u-X_l), & X_l \le X \le X_u, \\ 1, & X_u \le X. \end{cases} \tag{24}$$

The lower critical value X_l is taken equal to the Fermi velocity v_F, whose value is 0.26781 for our choice of constants,[23] and the upper critical value X_u is taken equal to $2v_F$. The calculated values of $d^2\sigma/dEd\Omega$ are relatively insensitive to the specific choices of X_l and X_u, as was verified by performing one calculation also with $X_l = 0.5v_F$ and $X_u = 1.5v_F$.

Finally, the total nucleon-nucleon cross section σ is represented by the empirical formula

$$\sigma=\left(40+\frac{10\xi-37}{3\xi^2-2\xi+1}+\frac{10}{\xi^2}\right)\text{mb}, \tag{25}$$

with

$$\xi = m_0 X/\text{GeV}. \tag{26}$$

For a target nucleon at rest, ξ is the momentum of the incident nucleon in units of GeV. Equation (25) reproduces the average value of the experimental proton-proton and neutron-proton total cross sections[16,24] over the entire range of interest with an accuracy of about 10%. The cross section σ enters the calculation only within the products $K\sigma$ and $K'\sigma$.

E. Solution of equations of motion

To solve the above equations, we have generalized to the case of two separate fluids the relativistic particle-in-cell finite-difference computing method[25] that was used to solve the equations of motion for the one-fluid model. This generalization incorporates many of the techniques that have been developed for solving multiphase fluid-dynamics problems at nonrelativistic velocities.[26] To facilitate comparisons with experimental results, the calculations are performed in the laboratory reference frame.

As before, we subdivide the space in and around the nuclei into cells with dimensions δx, δy, and δz. Both fluids are represented by discrete computational particles which move through these cells. The finite-difference approximations to spatial derivatives are expressed as cell-to-cell differences of averages over each cell.

A given collision corresponds to an initial-value problem, for which initial and boundary conditions are prescribed. The calculation then advances the field variables through a sequence of cycles, with a time interval δt. We generate the solution for enough elapsed time to determine the ultimate distribution (in energy and direction) of the outgoing matter.

The layout of the computational mesh and the numerical-solution procedure resemble closely techniques that have been described previously.[25] Therefore, we discuss here only those new features that are introduced by the presence of two separate fluids. Each calculational cycle proceeds through four phases.

Phase 1 consists of three steps. In the first step, we add to the momentum and energy in every cell the amounts

$$\delta\vec{M}_1 = -\omega R X^2 \gamma_1 \vec{v}_1/(Y+1), \tag{27}$$

$$\delta\vec{M}_2 = -\omega R X^2 \gamma_2 \vec{v}_2/(Y+1), \tag{28}$$

$$\delta E_1 = -\omega R X^2 \gamma_1/(Y+1)\,, \tag{29}$$

and

$$\delta E_2 = -\omega R X^2 \gamma_2/(Y+1)\,, \tag{30}$$

where

$$R = \alpha(X) D_c \delta t\,. \tag{31}$$

This step is operative only for dissipative interactions, having $\omega \neq 0$.

In the second step of phase 1, we add to the momentum and energy in every cell the amounts

$$\delta \vec{M}_1 = R(\gamma_2 \vec{v}_2 - \gamma_1 \vec{v}_1)\,, \tag{32}$$

$$\delta \vec{M}_2 = R(\gamma_1 \vec{v}_1 - \gamma_2 \vec{v}_2)\,, \tag{33}$$

$$\delta E_1 = R(\gamma_2 - \gamma_1)\,, \tag{34}$$

and

$$\delta E_2 = R(\gamma_1 - \gamma_2)\,. \tag{35}$$

These equations describe the conservative exchange of momentum and energy between the fields, which can be calculated either explicitly as shown, or implicitly. In the implicit case, the calculations can proceed even with infinite coupling (the one-fluid limit). In the explicit case this step of the calculation becomes unstable with strong coupling and/or with a large time step per cycle.

With implicit coupling, we define for fluid i the quantities

$$a_i = 1/[\gamma_i(\epsilon_i + p_i)] \tag{36}$$

and

$$b_i = \gamma_i/[\gamma_i^2 \epsilon_i + p_i(\gamma_i^2 - 1)]\,. \tag{37}$$

Denoting by a tilde the new value of a quantity, we write Eqs. (32)–(35) in the alternative form

$$\tilde{\vec{M}}_1 = \vec{M}_1 + R(a_2 \tilde{\vec{M}}_2 - a_1 \tilde{\vec{M}}_1)\,, \tag{38}$$

$$\tilde{\vec{M}}_2 = \vec{M}_2 + R(a_1 \tilde{\vec{M}}_1 - a_2 \tilde{\vec{M}}_2)\,, \tag{39}$$

$$\tilde{E}_1 = E_1 + R(b_2 \tilde{E}_2 - b_1 \tilde{E}_1)\,, \tag{40}$$

and

$$\tilde{E}_2 = E_2 + R(b_1 \tilde{E}_1 - b_2 \tilde{E}_2)\,. \tag{41}$$

These equations can be solved algebraically in pairs, with results that are bounded as $R \to \infty$. However, this formulation is only partially implicit, which gives rise to a potential disadvantage. In particular, the values of a_i and b_i are determined from the results of the previous cycle, and experience shows that the coupling between fields can accordingly be inaccurate in some circumstances. Weighing the advantages and disadvantages of both procedures, as determined by numerical testing, we have concluded that the explicit procedure is better, and have performed all calculations reported in this paper with that technique.

The third step in phase 1 converts the total-fluid quantities of Eqs. (14)–(16) to total-fluid pressures and velocities, and uses these to determine the pressures and velocities in each field by means of Eqs. (17) and (18). These new values replace the ones from the previous cycle for all purposes in the rest of the current cycle.

In phase 2, the pressure gradients acting on the two fields are used to change the momentum and energy of each, independently of the other, according to

$$\delta \vec{M}_1 = -(\nabla p_1)\delta t\,, \tag{42}$$

$$\delta \vec{M}_2 = -(\nabla p_2)\delta t\,, \tag{43}$$

$$\delta E_1 = -\nabla \cdot (p_1 \vec{v}_1)\delta t\,, \tag{44}$$

and

$$\delta E_2 = -\nabla \cdot (p_2 \vec{v}_2)\delta t\,. \tag{45}$$

The appropriate finite-difference expressions are given in detail in Ref. 25.

In phase 3, the computational particles describing the configuration of each field are moved with the velocities of that field, and the corresponding convective changes of N_1, N_2, $\vec{M}_1$, $\vec{M}_2$, E_1, and E_2 are calculated for all particles moving from one cell to another.[25]

In phase 4, we solve Eqs. (4)–(6) for n_i, ϵ_i, p_i, and $\vec{v}_i$ for each fluid, using exactly the same procedure as in Ref. 25.

III. CALCULATED RESULTS

A. Time evolution of the matter distribution

In the two-fluid model, the target and projectile are partially transparent to each other by an amount that depends upon the coupling between the two fluids. This is illustrated in Fig. 1 for the reaction $^{20}\mathrm{Ne} + {}^{238}\mathrm{U}$ at a laboratory bombarding energy per nucleon of 250 MeV and an impact parameter that is one-half the sum of the target and projectile radii. Each column presents a side view of the matter distribution evolving in time for a given value of the coupling. The initial frame in each case shows a ^{238}U target bombarded from above by a ^{20}Ne projectile, which is Lorentz-contracted in the incident direction.

The target is represented by light points, and the projectile is represented by heavy points. These points, or computational particles, are aligned so that in the direction perpendicular to the page only a single point is visible initially. However, as the impulse resulting from the collision propagates throughout the system, this alignment is destroyed and additional particles

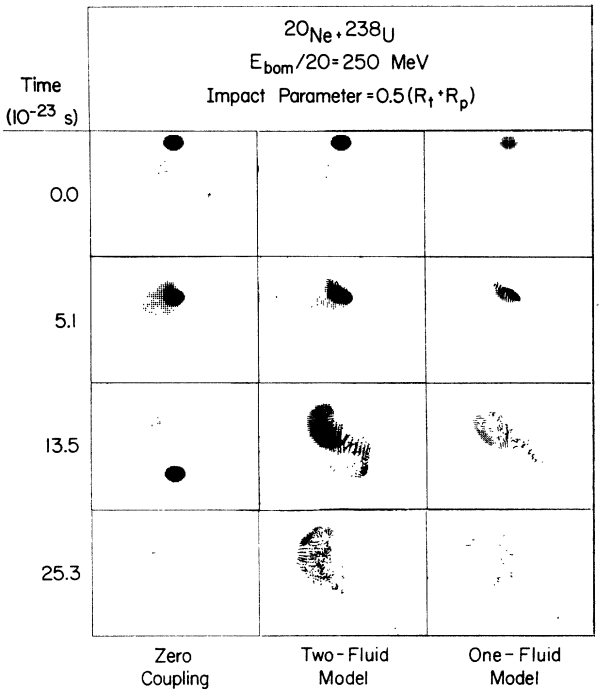

FIG. 1. Calculated time evolution of the matter distribution in the collision of ^{20}Ne with ^{238}U for three different values of the coupling between the two fluids. The left-hand column gives the result for zero coupling, where the target and projectile pass through each other without interaction. The middle column gives the result for a finite coupling taken from free nucleon-nucleon scattering, which corresponds to the present two-fluid model. The right-hand column gives the result for infinite coupling, which corresponds to the previous one-fluid model (Ref. 14). The impact parameter is 0.5 $(R_t + R_p) = 0.5\ (1.2049)(A_t^{1/3} + A_p^{1/3})$ fm, and the laboratory bombarding energy per nucleon is 250 MeV.

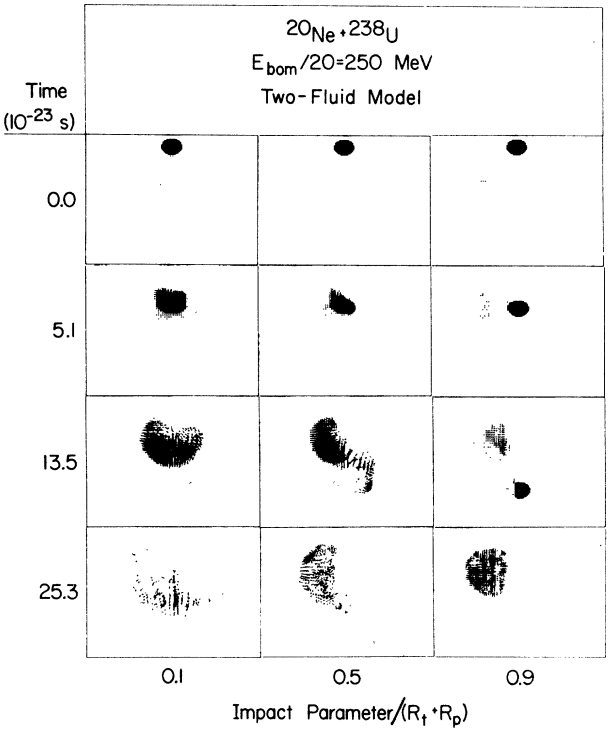

FIG. 2. Calculated time evolution of the matter distribution in the collision of ^{20}Ne with ^{238}U for three different impact parameters. The laboratory bombarding energy per nucleon is 250 MeV.

come into view. For the target we use $2^3 = 8$ particles per computational cell, whereas for the smaller, Lorentz-contracted projectile we use $3^3 = 27$ particles per cell. The radius of the target spans six cells, which means that the cells are 1.244 fm in each dimension. For the reaction illustrated in Fig. 1, this leads to 4420 computational particles for the half space in which the calculation is performed. Only half the problem is actually zoned, as we take advantage of the symmetry plane. For this reaction, the time step per cycle is taken to be 3.369×10^{-24} s.

For zero coupling, the target and projectile pass through each other without interaction, as shown in the left-hand column of Fig. 1. For a finite coupling taken from free nucleon-nucleon scattering, corresponding to our present two-fluid model, the target and projectile deform, compress, and excite each other during their interpenetration, as shown in the middle column. However, their deformation, compression, and excitation are less than those corresponding to the infinite coupling of the one-fluid model, as shown in the right-hand column. During the later stages of the process the results for the two-fluid model and the one-fluid model are qualitatively very similar, although the matter emerging in the backward direction is somewhat less for the two-fluid model than for the one-fluid model.

For this same reaction, we show in Fig. 2 the dependence of the results calculated in the two-fluid model upon the impact parameter. In nearly central collisions, the projectile deposits most of its kinetic energy and momentum in the target, which leads to a violent explosion of the system. At the other extreme, in peripheral collisions the projectile is fragmented into a portion that proceeds roughly straight ahead at its original velocity and another portion that deposits its kinetic energy and momentum in the target. This disturbs the target much less violently than in nearly central collisions, and its deformation, compression, and excitation are therefore much less.

The analogous solutions for a bombarding energy

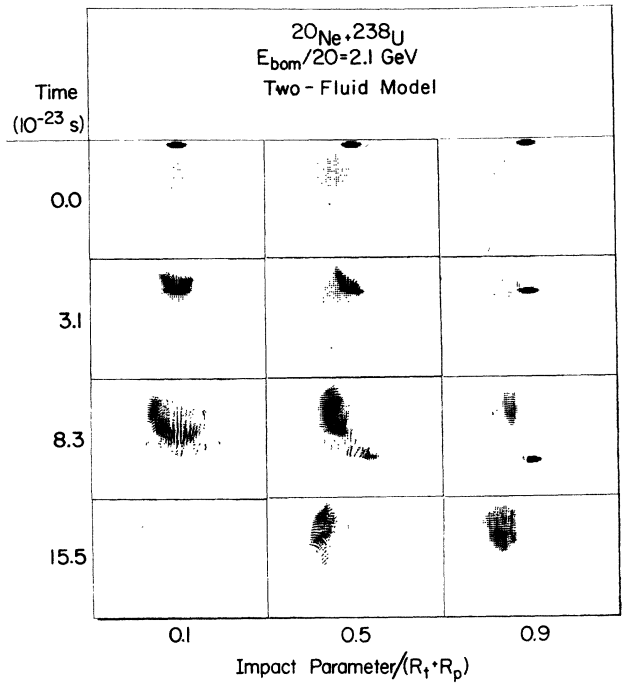

FIG. 3. Calculated time evolution of the matter distribution in the collision of ^{20}Ne with ^{238}U for three different impact parameters. The laboratory bombarding energy per nucleon is 2.1 GeV.

per nucleon of 2.1 GeV are shown in Fig. 3. Because of the higher bombarding energy, the Lorentz contraction of the projectile is more extreme and the entire process occurs more rapidly than before. The remaining features of the collision are qualitatively similar to those at the lower bombarding energy.

B. Numerical uncertainties

In any finite-difference solution of the equations of fluid dynamics, there are errors associated with the numerical approximations used. A principal goal is to minimize these errors, subject to the constraints of available computer time and memory. For problems in three spatial dimensions, these constraints become expecially severe because the computer time increases at least as fast as the fourth power of the number of finite-difference cells per dimension. Thus, a compromise is always required between the need for high resolution, on the one hand, and the limitations of the computer, on the other hand.

In the present investigations, the required sacrifice of accuracy is fairly severe. With six computational cells across the initial radius of the target nucleus, we lose significantly in the resolution of such details as shock structure, compressional spikes, surface effects, and coalescence into several-nucleon fragments. Because three-dimensional calculations with appreciably greater resolution are too costly to perform, we have compared the results of several one-dimensional calculations with both coarse and fine resolution. These one-dimensional calculations correspond to collisions of two slabs of nuclear matter whose thicknesses are finite but which extend to infinity in the two transverse directions.

Some of our present conclusions about numerical accuracy agree with our previous PIC-method experience for one-fluid studies.[13,14,25] This includes, for example, the tendency toward striation when the flow speeds are very low, as illustrated in the lower right-hand frame of Fig. 2. However, we also observe effects that are peculiar to the two-fluid model. In particular, a finely resolved two-fluid calculation produces a relatively gradual buildup of a narrow compressional spike in each material, in contrast to a broader shocked region in a one-fluid calculation. Although at the current stage of our investigations we can comment only in a preliminary way, the occurence of such fine-scale interaction profiles is of great interest and significance for at least four reasons:

(1) In nucleus-nucleus collisions, the narrow regions of high compression are somewhat narrower than expected on the basis of a one-fluid dynamical model. This reduces somewhat the probability of producing nuclear matter in a phase that is different from the ordinary phase.

(2) Two-fluid flow at relativistic speeds possibly exhibits some of the classic instabilities observed in nonrelativistic two-fluid flow, such as in a fluidized dust bed.[27,28] Thus, a study of such flows has potential interest beyond the context of the present investigation, as well as having implications relative to the nature of the breakup in nucleus-nucleus collisions.

(3) The presence of narrow compressional spikes is discouraging from the viewpoint of an accurate numerical resolution of the collisions. Consider the formation and subsequent reexpansion of (a) a very narrow region of high density and pressure and (b) a relatively broad region of somewhat lower density and pressure. The first of these represents the accurate solution of a three-dimensional calculation, whereas the second is what occurs in a coarsely resolved calculation, where one computational cell is appreciably larger than the cross section of a compressional spike. The energy and angular distributions of the outgoing matter must differ to some degree in these two cases. We speculate that if the nuclear equation of state were linear in the compression,

the two cases would produce closely similar results. However, our nuclear equation of state is strongly nonlinear, and we have no convincing evidence regarding the extent of the discrepancy between our poorly resolved approximation and the accurate solution.

(4) We have subjected the well-resolved one-dimensional calculations to a symmetry test, with encouraging results. With the target at rest in the collision of two slabs of matter whose thicknesses correspond to ^{238}U nuclei, we examine the midline representation of the collision. After performing a Lorentz transformation to the center-of-mass system, we found an excellent degree of symmetry about the collision point. This test result, along with a late-time three-dimensional symmetry test result for the coarsely resolved uranium-uranium system to be discussed later, are necessary, if not sufficient, indications that the calculations are numerically reliable.

As these remarks indicate, much remains to be done before our calculations are fully understood, with regard to both their numerical accuracy and their physical implications. Nevertheless, it is worthwhile to compare our present results with experimental data and to see what can be learned. It is to this task that we now turn.

C. Comparison of calculated energy spectra with experimental data

For a given impact parameter we construct from the velocity vectors at some large time the double differential quantity $d^2N_{\rm mat}/dEd\Omega$ for the outgoing matter. The small amount of matter that already has passed through the top and side boundaries of the computational mesh is also included. In an effort to improve the numerical accuracy, we average the results of the last 11 cycles out of a total of 150 cycles, but this averaging has little effect. The accuracy of our results is limited primarily by statistical errors arising from the finite number of computational particles employed and by striation and other finite-difference errors in the numerical solutions themselves.

To obtain the double differential cross section $d^2\sigma_{\rm mat}/dEd\Omega$ for the outgoing matter, we integrate the values of $d^2N_{\rm mat}/dEd\Omega$ over impact parameter by use of a five-point trapezoidal approximation, taking into account the linear weighting with impact parameter. Under the assumption that the charge is distributed uniformly throughout the entire matter, we then obtain the double differential cross section $d^2\sigma/dEd\Omega$ for outgoing charged particles by multiplying $d^2\sigma_{\rm mat}/dEd\Omega$ by $(Z_t+Z_p)/(A_t+A_p)$.

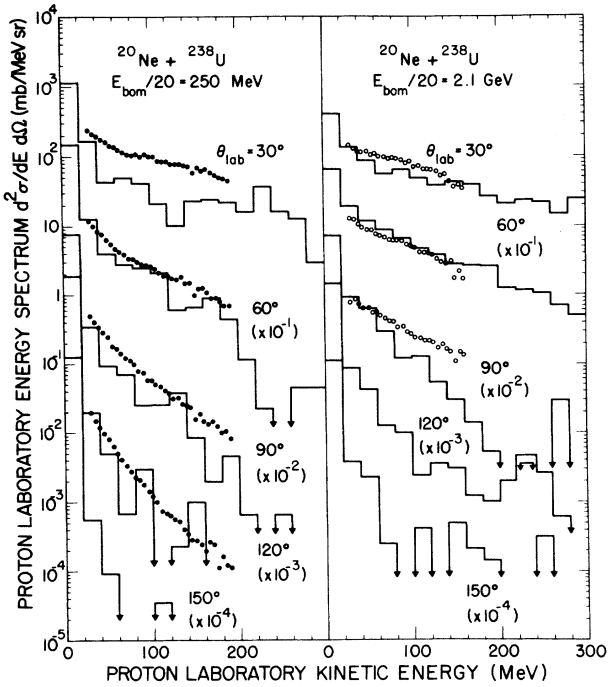

FIG. 4. Comparison of calculated and experimental energy spectra for outgoing charged particles from the collision of ^{20}Ne with ^{238}U. The histograms give the calculated results, and the points give the experimental results (Ref. 29). The solid points in the left-hand column, where the laboratory bombarding energy per nucleon is 250 MeV, are expected to be accurate to within 35% and include contributions from outgoing protons, deuterons, tritons, ^{3}He particles, and ^{4}He particles. The open points in the right-hand column, where the laboratory bombarding energy per nucleon is 2.1 GeV, are uncertain by a factor of 2 and include contributions from outgoing protons, tritons, ^{3}He particles, and ^{4}He particles (but not deuterons).

The resulting values of $d^2\sigma/dEd\Omega$ for ^{20}Ne + ^{238}U at laboratory bombarding energies per nucleon of 250 MeV and 2.1 GeV are shown in Fig. 4 in the form of energy spectra at five laboratory angles ranging from 30° to 150°. Some idea of the numerical accuracy of the calculations can be obtained from the fluctuations in the histograms, which are obtained using angular bins of 10° width. These calculated results are compared with the recent experimental data of Gosset *et al.*[29] for outgoing charged particles. The experimental results for a bombarding energy per nucleon of 250 MeV include contributions from outgoing protons, deuterons, tritons, ^{3}He particles, and ^{4}He particles, whereas those for a bombarding energy per nucleon of 2.1 GeV include contributions from protons, tritons, ^{3}He particles, and ^{4}He particles (but not deuterons). The former experimental results are expected to

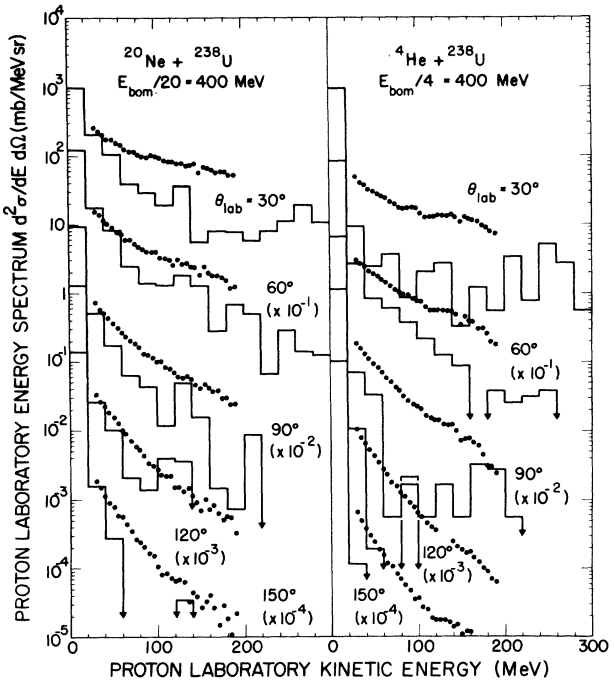

FIG. 5. Comparison of calculated and experimental energy spectra for outgoing charged particles from the collision of ^{20}Ne (left-hand column) and ^{4}He (right-hand column) with ^{238}U. The laboratory bombarding energy per nucleon is 400 MeV. The histograms give the calculated results, and the solid points give the experimental results, which are expected to be accurate to within 35% and include contributions from outgoing protons, deuterons, tritons, ^{3}He particles, and ^{4}He particles (Ref. 29).

be accurate to within 35%, whereas the latter are uncertain by a factor of 2. Particles heavier than protons were not detected experimentally at energies as high as those for protons. To obtain the relatively small high-energy contributions from these heavier particles, we extrapolated the logarithm of the measured yield linearly in energy.

At a bombarding energy per nucleon of 250 MeV, the calculations reproduce correctly the experimental slopes at each angle, as well as the overall decrease in the experimental cross section when going from forward to backward angles. However, the calculated values at 30° are only one-third the experimental values. At a bombarding energy per nucleon of 2.1 GeV, the calculations reproduce correctly the experimental data to within their uncertainties for 30° and 60° at all energies and for 90° at low energies. However, for 90° at high energies, the calculated values are only one-fourth the experimental values.

Compared to the previous results calculated with the one-fluid model,[14,15] the present results calculated with the two-fluid model are somewhat smaller in the backward directions. This is because in the present calculations the target and projectile are partially transparent to each other, which reduces the compressional energy and excitation energy that is available for ejecting particles backward during the later expansion stage. In the forward directions, the results of the two models are approximately the same, although even here the values calculated with the two-fluid model are slightly smaller than those calculated with the one-fluid model, to within the numerical uncertainties of the calculations. The reason for this is that with zero coupling the only forward component is the whole projectile; with small coupling the projectile is

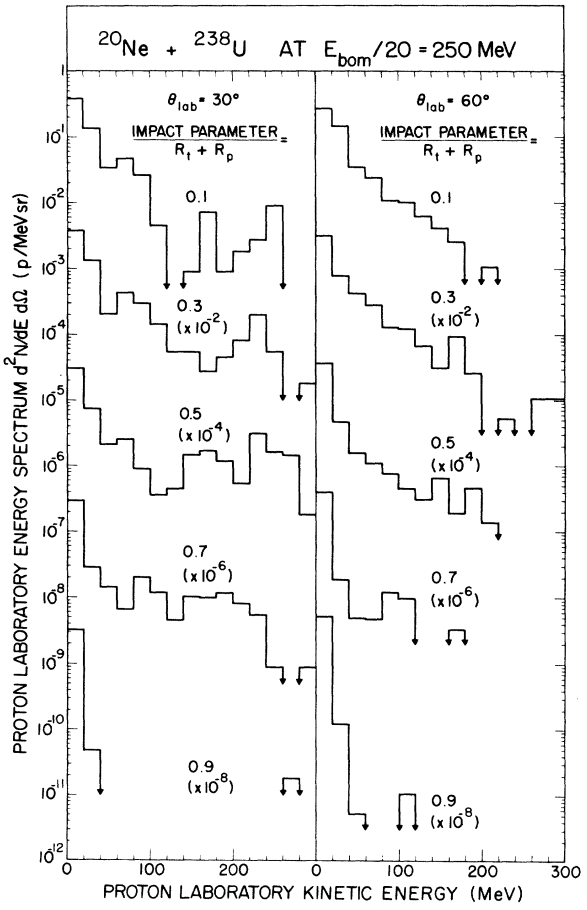

FIG. 6. Calculated energy spectra for outgoing charged particles from the collision of ^{20}Ne with ^{238}U at five different impact parameters. The laboratory bombarding energy per nucleon is 250 MeV. The laboratory angle is 30° in the left-hand column and is 60° in the right-hand column.

dispersed and the target contributes only low-energy outgoing particles.

Similar comparisons are presented in Fig. 5 for the reactions $^{20}Ne + ^{238}U$ and $^{4}He + ^{238}U$ at a bombarding energy per nucleon in each case of 400 MeV. The experimental data[29] include contributions from outgoing protons, deuterons, tritons, ^{3}He particles, and ^{4}He particles, and are expected to be accurate to within 35%. For $^{20}Ne + ^{238}U$ the calculations reproduce correctly the experimental slopes at each angle, as well as the overall decrease in the experimental cross section when going from forward to backward angles. However, the calculated values are slightly below the experimental values in the backward directions and are only one-third the experimental values in the forward directions. For $^{4}He + ^{238}U$, the calculated values at all angles are substantially smaller than the experimental values.

In an attempt to understand the discrepancy between the calculated and experimental results in the forward directions, we show in Fig. 6 the dependence of the energy spectra at 30° and 60° upon impact parameter for $^{20}Ne + ^{238}U$ at a laboratory bombarding energy per nucleon of 250 MeV. At 60° the spectra decrease approximately exponentially with increasing energy for all impact parameters. However, at 30° there are also small peaks in the energy spectra near 250 MeV. For moderate and large impact parameters these peaks arise from projectile fragmentation, but for nearly central collisions they are associated instead with the expansion of the projectile following its compression and excitation as it passes through the target.

D. Predictions for $^{238}U + ^{238}U$

As seen in the previous subsection, the accuracy with which the two-fluid model describes the experimental data increases as we progress from the light projectile ^{4}He to the somewhat heavier projectile ^{20}Ne. This is probably because ^{20}Ne has more degrees of freedom and also a smaller surface region compared to volume region than does ^{4}He. However, it could also be associated with the larger total kinetic energy and momentum transferred to the target from a ^{20}Ne projectile compared to a ^{4}He projectile, since our particular finite-difference method of solution does not behave as well in the perturbed stagnation resulting from small impulses. This could also explain why for $^{20}Ne + ^{238}U$ the two-fluid model works better when the bombarding energy per nucleon is 2.1 GeV than when it is 250 or 400 MeV.

For these reasons, we expect the two-fluid model to become increasingly satisfactory as the size of the projectile increases. We therefore show in Fig. 7 the caluclated energy spectra for collisions of ^{238}U with ^{238}U at bombarding energies per nucleon of 250 MeV and 2.1 GeV.

These distributions may be considered as theoretical background estimates, in the sense that they are based on straightforward extrapolations of conventional ideas concerning nuclear physics. While agreement between theory and experiment would not necessarily mean that the conventional picture is correct, dramatic disagreement should lead to new information. Apart from possible numerical inaccuracies, the main uncertainty in these results is their sensitivity to the choice of the nuclear equation of state, since we have yet to vary that. Thus, it is conceivable that the original goal of this program—experimental determination of the nuclear equation of state at high density—may be realized when data on $^{238}U + ^{238}U$ (or comparable) collisions become available.

The main qualitative difference between the calculated cross sections for $^{20}Ne + ^{238}U$ and for $^{238}U + ^{238}U$ is as expected. The latter are larger and decrease less rapidly with increasing proton energy, showing that a ^{238}U projectile imparts

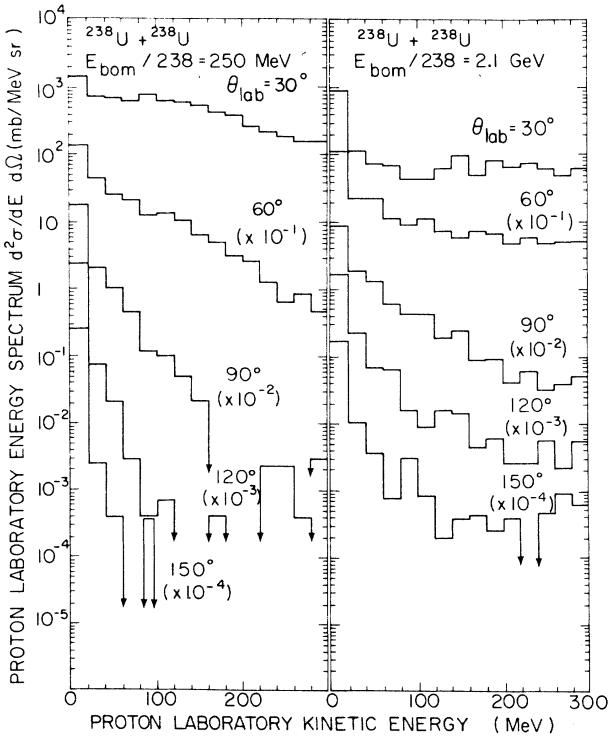

FIG. 7. Calculated energy spectra for outgoing charged particles from the collision of ^{238}U with ^{238}U. The laboratory bombarding energy per nucleon is 250 MeV in the left-hand column and is 2.1 GeV in the right-hand column.

more energy than a ^{20}Ne projectile to the nucleons in a ^{238}U target.

In the absence of experimental data, we have two checks on the numerical accuracy of the calculations, in addition to the above qualitative remark. The first is forward-backward symmetry in the center-of-mass frame of the invariant differential cross section

$$(E+m_0)d^2\sigma/d^3p = p^{-1}d^2\sigma/dEd\Omega\,, \tag{46}$$

where p is the momentum of a proton with kinetic energy E and mass m_0. Careful examination of the calculated cross sections for ^{238}U+^{238}U at $E_{\rm bom}/238 = 250$ MeV shows that the symmetry is good to an accuracy of about 20%. In view of the coarseness required for a practical numerical calculation, this agreement is better than anticipated.

Our study of this symmetry leads us to endorse the view of many others, that in place of E and θ more appropriate variables are the rapidity

$$y = \ln[(m_0+E+p\cos\theta)/(m_0^2+p^2\sin^2\theta)^{1/2}] \tag{47}$$

and the transverse momentum normalized to mass[30]

$$\nu = p\sin\theta/m_0\,. \tag{48}$$

In the nonrelativistic limit, these quantities become the velocity components parallel to the beam and perpendicular to the beam, respectively. However, the rapidity has the advantage of being linear even in the relativistic regime. That is, the rapidity of a particle measured by an observer moving in the direction of the beam is simply the rapidity measured in the laboratory frame minus the rapidity measured by the observer,

$$y_{\rm obs} = \tanh^{-1}v_{\rm obs}\,. \tag{49}$$

Thus, in a plot of invariant cross section versus y and ν, the requirement for center-of-mass-frame symmetry becomes

$$\sigma(y_C+\Delta,\nu) = \sigma(y_C-\Delta,\nu)\,. \tag{50}$$

Such a plot for ^{238}U+^{238}U at $E_{\rm bom}/238 = 250$ MeV is shown in Fig. 8. Aside from demonstrating the symmetry of the calculated cross section, this figure shows how points corresponding to rectangular bins in E and θ are distributed on a $y-\nu$ grid. Evidently, it should be easier to analyze comparisons between experiment and theory when both are plotted versus y and ν instead of E and θ. However, this approach does pose practical difficulties in transforming experimental data.

A second theoretical check on our calculation is a comparison of the results with those in the firestreak model of Myers.[31] In that model, narrow imaginary tubes are drawn parallel to the beam direction. Projectile and target segments in each tube do not interact with material in neighboring tubes. Instead, the matter in each tube comes to equilibrium, making a hot medium which decays by isotropic emission in the center-of-mass frame of that tube. Thus, the dynamics are simplified considerably relative to our model, facilitating not only the prediction of cross sections, but also the inclusion of the nuclear surface diffuseness. The firestreak results for ^{238}U+^{238}U collisions are relatively insensitive to the surface diffuseness and are in good agreement with the hydrodynamic results.[32-34] This suggests that both calculations give fairly accurate background estimates and that the gross features are determined largely by energy and momentum conservation.

At the lower bombarding energy per nucleon of 250 MeV, the accuracy of the agreement between the two-fluid dynamical model and the firestreak model is about 20%.[32,33] At the higher bombarding energy per nucleon of 2.1 GeV, the agreement is not as good. For outgoing protons with energy per nucleon $\gtrsim$200 MeV, firestreak calculations with and without assuming pions in equilibrium with the nucleons differ from each other by factors as large as 3 or 4, whereas the

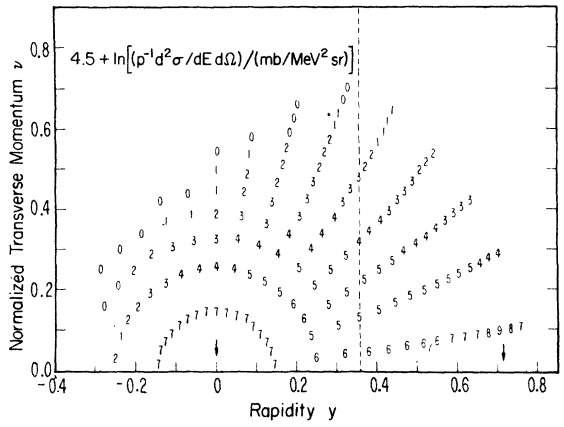

FIG. 8. Lorentz-invariant inclusive differential cross section for outgoing charged particles from the collision of ^{238}U with ^{238}U versus rapidity y and normalized transverse momentum ν, defined by Eqs. (47) and (48), respectively. The laboratory bombarding energy per nucleon is 250 MeV. The numbers in the plot give the values of $4.5+\ln[(p^{-1}d^2\sigma/dEd\Omega)/(\text{mb/MeV}^2\,\text{sr})]$, rounded to the nearest integer, for all values greater than zero. The dashed vertical line is the expected axis of reflection symmetry, corresponding to the center-of-mass rapidity. The arrows indicate the target and beam rapidities.

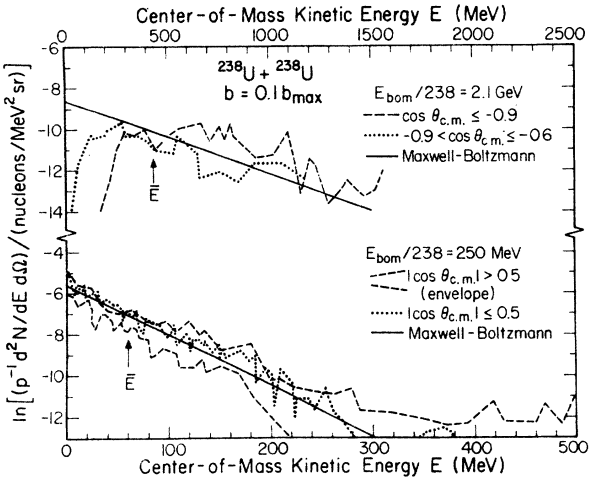

FIG. 9. Test of isotropy and thermalization of outgoing charged particles from the nearly head-on collision of ^{238}U with ^{238}U, for which the impact parameter $b = 0.1\,b_{max} = 0.1(R_t + R_p)$. The laboratory bombarding energy per nucleon is 250 MeV in the lower portion of the figure and is 2.1 GeV in the upper portion. In each case, the natural logarithm of the invariant double differential distribution $p^{-1}d^2N/dEd\Omega$ is plotted versus the center-of-mass kinetic energy for two different angular ranges. The solid straight line in each case gives the Maxwell-Boltzmann distribution obtained by equipartitioning the initial collision energy among the three translational degrees of freedom of each nucleon in the system. This leads to a nuclear temperature of 39.6 MeV in the lower portion of the figure and 234 MeV in the upper portion. The corresponding mean kinetic energies per nucleon are indicated by the arrows. Note that the energy scales are different for the lower and upper portions of the figure.

results of the no-pion assumption generally agree with those of hydrodynamics to within a factor of 2.[33,34] Because the inclusion of pion degrees of freedom in the two-fluid model would correspond to a softer nuclear equation of state than that used here, the trend of the comparisons with the firestreak results is qualitatively reasonable and strengthens the hope that the equation of state has a significant effect on the inclusive proton spectra.

However, there remains a serious question: To what extent may the integration over impact parameter mask significant discrepancies? Because the most interesting effects should occur for nearly central collisions, we focus on them. For a head-on collision, the firestreak model, like the earlier fireball model,[29,35] predicts complete isotropy of emitted protons in the ^{238}U + ^{238}U center-of-mass frame. In Fig. 9 we present our results for impact parameter $b = 0.1b_{max}$.

As seen in Fig. 9, for a bombarding energy per nucleon of 250 MeV, our two-fluid model predicts a center-of-mass invariant distribution that is nearly isotropic and that decreases nearly exponentially with increasing energy. Furthermore, both the magnitude and slope are very similar to those for a Maxwell-Boltzman distribution whose temperature is 39.6 MeV, corresponding to complete thermalization and equipartition of energy into the three translational degrees of freedom of each nucleon in the system. There may be significant departures for nucleons with energy between about 35 and 55 MeV, but otherwise the agreement is as good as fluctuations (presumably due to the coarseness of the numerical procedures) permit.

On the other hand, the calculated results for a bombarding energy per nucleon of 2.1 GeV clearly violate both isotropy and thermalization. Unlike a thermal distribution, our calculated distributions decrease significantly near zero energy. Furthermore, for higher energies the calculated distribution is larger near the backward direction than at other angles. This calculation confirms the earlier indication[15] that a single-particle-inclusive distribution, for events corresponding to nearly head-on collisions, could be sensitive to the nature of the collision process.

E. Maximum compression and excitation

A major purpose of investigating high-energy nuclear collisions is to learn about the response of nuclear matter to substantial compression and excitation. In the one-fluid model, one can solve for the maximum rest-frame compression,[14] compressional energy per nucleon, and internal excitation energy per nucleon exactly in terms of the nuclear equation of state and the bombarding energy per nucleon. This is done by integrating the equations of motion over an infinitesimal volume near the contact point in a head-on collision. In this case the kinetic energy in the center-of-velocity frame is converted entirely into compressional energy and internal excitation energy.

For our nuclear equation of state and a laboratory bombarding energy per nucleon of 250 MeV (corresponding to a center-of-velocity bombarding energy per nucleon of 60.5 MeV), the one-fluid model gives a maximum rest-frame compression of 2.24, a maximum compressional energy per nucleon of 23.4 MeV, and a maximum internal excitation energy per nucleon of 37.1 MeV. For a laboratory bombarding energy per nucleon of 2.1 GeV (corresponding to a center-of-velocity bombarding energy per nucleon of 427 MeV), these values are 3.66, 101 MeV, and 326 MeV, respectively. (The maximum compressions given in

Refs. 13 and 14 refer to center-of-velocity bombarding energies per nucleon rather than to laboratory bombarding energies per nucleon.)

The maximum compression and excitation are achieved only for an infinitesimal time in an infinitesimal volume near the contact point. As time proceeds, the maximum compression and excitation are reduced substantially because of the divergence of the shock waves and the rarefaction from the trailing surface of the projectile.

In the two-fluid model, the interpenetration of the target and projectile leads to a gradual rather than a sudden conversion of kinetic energy into compressional energy and internal excitation energy. We are unable to solve exactly the coupled equations of motion in the two-fluid model to obtain the maximum compression and excitation. Also, the finite resolution imposed by our moderately coarse three-dimensional computational grid does not allow us to answer this question. We have therefore solved numerically in one dimension the collision of two slabs of matter whose thicknesses correspond to ^{238}U nuclei; the slabs extend to infinity in the two transverse directions. For this one-dimensional calculation, the length of our cells is one-fifth that in the three-dimensional calculations, and there are 10 times as many particles per cell. The time step is about one-fifth that used in the three-dimensional calculations.

For large relative velocities of the two fluids, where $X > X_u$ and the target and projectile fluids have not yet begun to merge, it is appropriate to consider the compression and excitation of each fluid separately. When the bombarding energy per nucleon is 250 MeV, the two fluids begin to merge after about 1.0×10^{-23} s, at which time the rest-frame compression of each fluid is about 1.2, the compressional energy per nucleon is about 0.4 MeV, and the internal excitation energy per nucleon is about 20 MeV.

For this bombarding energy per nucleon of 250 MeV, the maximum compression is reached after about 2.0×10^{-23} s (in one particular cell), at which time the rest-frame compression of each fluid is about 1.3, the compressional energy per nucleon is about 1.1 MeV, and the internal excitation energy per nucleon is about 30 MeV. The two fluids are now partially mixed, and if we alternatively view them as a single fluid, the rest-frame compression is about 2.6. This value is maintained, with some fluctuations, for about 10^{-22} s. At this density the compressional energy per nucleon is about 38 MeV, which would require a negative internal excitation energy per nucleon (about −7 MeV) to satisfy energy conservation.

Such a negative internal excitation energy is, of course, physically impossible. It arises because the actual transition from two fluids at high relative velocities to a single fluid at low relative velocities is more complicated than the smooth interpolation that we have used here. Within our present framework, an upper limit to the maximum compression may be obtained by requiring that the total available energy per nucleon be converted entirely into compressional energy. At this bombarding energy per nucleon of 250 MeV, where the total available energy per nucleon is about 31.1 MeV, this procedure yields an upper limit of about 2.4 for the maximum compression. On the other hand, within a broader framework that allows for the possibility of a different phase of nuclear matter at a sufficiently low energy per nucleon, the original estimate of about 2.6 for the maximum compression would be applicable. (This estimate depends very little on the precise form of the equation of state for high compressions, since it is obtained by simply doubling the compression achieved by each fluid separately.)

An analogous situation prevails at higher bombarding energies, although the compression is much larger. For example, when the bombarding energy per nucleon is 2.1 GeV, the two fluids begin to merge after about 2.2×10^{-23} s, at which time the rest-frame compression of each fluid is about 2.3, the compressional energy per nucleon is about 25 MeV, and the internal excitation energy per nucleon is about 250 MeV.

For this bombarding energy per nucleon of 2.1 GeV, the maximum compression is reached after about 6.3×10^{-23} s, at which time the rest-frame compression of each fluid is about 4, the compressional energy per nucleon is about 130 MeV, and the internal excitation energy per nucleon is about 200 MeV. In this case the two fluids have completely merged according to our criterion of $X < X_l$, and the combined rest-frame compression is about 8. However, this value is maintained for only about 5×10^{-24} s. At this density the compressional energy per nucleon is about 610 MeV, which would require a negative internal excitation energy per nucleon (about −280 MeV) to satisfy energy conservation.

As before, such a compression would be possible within a broader framework that allows for the possibility of a different phase of nuclear matter at a sufficiently low energy per nucleon. However, within our current framework, the requirement that the total available energy per nucleon of about 330 MeV be converted entirely into compressional energy yields an upper limit of about 6 for the maximum compression.

In contrast to the predictions of the conventional

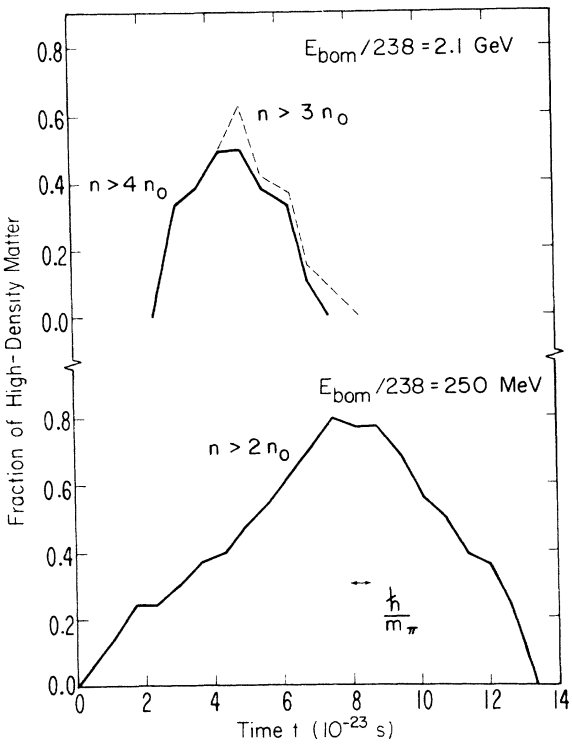

FIG. 10. Fraction of nuclear matter with rest-frame compression greater than a specified value versus time, for the collision of two nuclear slabs whose initial density is n_0 and whose thickness is equal to the diameter of a ^{238}U nucleus. The lower portion of the figure refers to a bombarding energy per nucleon of 250 MeV and to $n > 2n_0$. The upper portion refers to a bombarding energy per nucleon of 2.1 GeV; the dashed line corresponds to $n > 3n_0$ and the solid line corresponds to $n > 4n_0$. The duration of a pion time unit, $\hbar/m_\pi$, is indicated to suggest a relevant time scale.

one-fluid dynamical model—where the compression of nuclear matter is accompanied by a relatively large internal excitation energy—our two-fluid dynamical model suggests that it may be possible to compress nuclear matter while introducing little internal excitation energy. Provided that there is a different phase of nuclear matter at a lower energy per nucleon than the ordinary phase, this would in general increase the probability of a transition to that phase.

An alternative measure of compression that may be more reliable and more informative than the maximum value is the amount of nuclear material contained in a region of density above a specified multiple of n_0, the normal density. Figure 10 gives this amount as a function of time for ^{238}U projectile slabs incident on stationary ^{238}U target slabs at bombarding energies per nucleon of 250 MeV and 2.1 GeV. These graphs were constructed by first finding the number of adjacent computational cells with rest-frame density n greater than $2n_0$ for $E_{bom}/238 = 250$ MeV or greater than either $3n_0$ or $4n_0$ for $E_{bom}/238 = 2.1$ GeV. These values were then divided by the total number of cells (120) in two ^{238}U slabs at rest, and were finally multiplied by a factor to take into account the average density in the computational frame. These factors are 2.25 for $n > 2n_0$ at $E_{bom}/238 = 250$ MeV, 5.10 for $4n_0 \geq n > 3n_0$ at $E_{bom}/238 = 2.1$ GeV, and 6.55 for $n > 4n_0$ at $E_{bom}/238 = 2.1$ GeV.

From Fig. 10 one sees that for a bombarding energy per nucleon of 250 MeV, more than 0.75 of the nuclear matter is contained in the $n > 2n_0$ region. For a bombarding energy per nucleon of 2.1 GeV, the corresponding values are about 0.50–0.55 for $n > 3n_0$ and are about 0.45 for $n > 4n_0$. These fractions are maintained for several times 10^{-23} s at the lower energy, and for about 10^{-23} s at the higher energy. These are clearly significant bulk densities and duration times, which could be even larger for a softer equation of state.

IV. SUMMARY AND CONCLUSION

We have introduced a two-fluid dynamical model that is designed to take into account the expected partial transparency of nuclei during collisions at high energy. The coupling between the target and projectile fluids was obtained from the cross section and momentum transfer for individual nucleon-nucleon collisions. At low relative velocities the two fluids merge, in which case the conventional one-fluid dynamical model is recovered.

For a given nuclear equation of state, we calculated with this two-fluid model the double differential cross section $d^2\sigma/dEd\Omega$ for outgoing charged particles from four reactions that have been studied experimentally. For the collision of the light projectile ^{4}He with ^{238}U, the results of the two-fluid model are substantially smaller than the experimental values at all energies and angles. For the collision of the somewhat heavier projectile ^{20}Ne with ^{238}U, at bombarding energies per nucleon of 250 and 400 MeV, the two-fluid model describes the overall features of the experimental data adequately, but at 30° the calculated values are only one-third the experimental values. At the higher bombarding energy per nucleon of 2.1 GeV, the two-fluid model describes the experimental data adequately in the forward directions and at 90° for low energies, but at 90° for high energies the calculated values are only one-fourth the experimental values.

The accuracy with which the two-fluid model

describes the experimental data therefore increases as we go to heavier projectiles and as we increase the bombarding energy. This is probably because a heavier projectile (1) has more degrees of freedom, (2) has a smaller surface region compared to volume region, and (3) deposits a larger total kinetic energy and momentum than a light projectile. Because of this, we calculated the cross section $d^2\sigma/dEd\Omega$ for outgoing charged particles from collisions of ^{238}U with ^{238}U, as predictions for future experiments.

By means of a one-dimensional calculation, we also studied the maximum compression and excitation that can be achieved in such collisions. At a bombarding energy per nucleon of 250 MeV, the maximum rest-frame compression of each separate fluid is about 1.3, which leads to a maximum rest-frame compression for the combined fluid of about 2.4 to 2.6. At a bombarding energy per nucleon of 2.1 GeV, the maximum rest-frame compression of each separate fluid is about 4, which leads to a maximum rest-frame compression for the combined fluid of about 6 to 8. When the fluids are viewed as separate, the compressional energy is relatively small compared to the internal excitation energy. However, when the fluids have merged into a single fluid, the available energy is primarily in the form of compressional energy.

The discrepancies between the calculated and experimental results for ^{20}Ne + ^{238}U at bombarding energies per nucleon of 250 and 400 MeV may arise from deficiencies in the two-fluid model, from inaccuracies in our numerical procedures, or from errors in the experimental data. On the other hand, perhaps the nuclear equation of state is significantly different from the one that we are currently using. As mentioned earlier, relativity alone implies modifications at high densities. Also, perhaps the interaction of nucleons inside a nuclear medium is significantly different from the free-nucleon-nucleon interaction that we are currently using. Or perhaps the formation of a new phase of nuclear matter alters substantially the evolution of the matter distribution. These possibilities clearly deserve further exploration.

We are grateful to G. F. Bertsch, S. E. Koonin, M. Gyulassy, J. W. Negele, and R. C. Slansky for comments concerning this work, as well as to A. M. Poskanzer and G. D. Westfall for providing us with a tabulation of the data of Ref. 29 prior to publication.

---

*This work was supported by the U. S. Energy Research and Development Administration.

†Permanent address: Institute for Theoretical Physics, State University of New York at Stony Brook, Stony Brook, New York 11794.

[1]S. Z. Belenkij and L. D. Landau, Usp. Fiz. Nauk 56, 309 (1955); Nuovo Cimento Suppl. 3, 15 (1956); in *Collected Papers of L. D. Landau*, edited by D. ter Haar (Gordon and Breach, New York, 1967), 2nd printing, Paper No. 88, p. 665.

[2]A. E. Glassgold, W. Heckrotte, and K. M. Watson, Ann. Phys. (N.Y.) 6, 1 (1959).

[3]G. F. Chapline, M. H. Johnson, E. Teller, and M. S. Weiss, Phys. Rev. D 8, 4302 (1973).

[4]C. Y. Wong and T. A. Welton, Phys. Lett. 49B, 243 (1974).

[5]W. Scheid, H. Müller, and W. Greiner, Phys. Rev. Lett. 32, 741 (1974).

[6]H. G. Baumgardt, J. U. Schott, Y. Sakamoto, E. Schopper, H. Stöcker, J. Hofmann, W. Scheid, and W. Greiner, Z. Phys. A273, 359 (1975).

[7]J. Hofmann, H. Stöcker, U. Heinz, W. Scheid, and W. Greiner, Phys. Rev. Lett. 36, 88 (1976).

[8]A. Y. Abul-Magd, Phys. Rev. C 12, 343 (1975).

[9]Y. Kitazoe, M. Sano, and H. Toki, Nuovo Cimento Lett. 13, 139 (1975).

[10]Y. Kitazoe, K. Matsuoka, and M. Sano, Prog. Theor. Phys. 56, 860 (1976).

[11]M. I. Sobel, P. J. Siemens, J. P. Bondorf, and H. A. Bethe, Nucl. Phys. A251, 502 (1975).

[12]G. F. Bertsch, Phys. Rev. Lett. 34, 697 (1975).

[13]A. A. Amsden, G. F. Bertsch, F. H. Harlow, and J. R. Nix, Phys. Rev. Lett. 35, 905 (1975).

[14]A. A. Amsden, F. H. Harlow, and J. R. Nix, Phys. Rev. C 15, 2059 (1977).

[15]A. A. Amsden, J. N. Ginocchio, F. H. Harlow, J. R. Nix, M. Danos, E. C. Halbert, and R. K. Smith, Jr., Phys. Rev. Lett. 38, 1055 (1977).

[16]O. Benary, L. R. Price, and G. Alexander, Lawrence Berkeley Laboratory Report No. UCRL-20000 NN, 1970 (unpublished).

[17]A. M. Poskanzer, G. W. Butler, and E. K. Hyde, Phys. Rev. C 3, 882 (1971).

[18]L. P. Remsberg and D. G. Perry, Phys. Rev. Lett. 35, 361 (1975).

[19]W. Busza, in *Proceedings of the International Conference on High-Energy Physics and Nuclear Structure, Santa Fe and Los Alamos, New Mexico*, 1975, edited by D. E. Nagle, A. S. Goldhaber, C. K. Hargrove, R. L. Burman, and B. G. Storms (American Institute of Physics, New York, 1975), p. 211.

[20]L. D. Landau and E. M. Lifshitz, *Fluid Mechanics*, translated by J. B. Sykes and W. H. Reid (Pergamon, London/Addison-Wesley, Reading, 1959), Chap. XV, pp. 499–506.

[21]C. Møller, K. Dan. Vidensk. Selsk. Mat.-Fys. Medd. 23, No. 1 (1945).

[22]R. M. Edelstein, E. J. Makuchowski, C. M. Meltzer, E. L. Miller, J. S. Russ, B. Gobbi, J. L. Rosen, H. A. Scott, S. L. Shapiro, and L. Strawczynski, Phys. Rev. Lett. 38, 185 (1977).

[23]W. D. Myers and W. J. Swiatecki, Ann. Phys. (N.Y.)

55, 395 (1969).
[24]T. G. Trippe, A. Barbaro-Galtieri, R. L. Kelly, A. Rittenberg, A. H. Rosenfeld, G. P. Yost, N. Barash-Schmidt, C. Bricman, R. J. Hemingway, M. J. Losty, M. Roos, V. Chaloupka, and B. Armstrong, Rev. Mod. Phys. 48, S1 (1976).
[25]F. H. Harlow, A. A. Amsden, and J. R. Nix, J. Comp. Phys. 20, 119 (1976).
[26]F. H. Harlow and A. A. Amsden, J. Comp. Phys. 18, 440 (1975).
[27]J. D. Murray, J. Fluid Mech. 21, 465 (1965).
[28]J. D. Murray, J. Fluid Mech. 22, 57 (1965).
[29]J. Gosset, H. H. Gutbrod, W. G. Meyer, A. M. Poskanzer, A. Sandoval, R. Stock, and G. D. Westfall, Phys. Rev. C 16, 629 (1977).
[30]Rapidity y and transverse momentum p_T have been used widely in descriptions of high-energy collisions of elementary particles. A modification appropriate to the nuclear case is to divide p_T by the mass of a nuclear fragment, giving the quantity ν of Eq. (48). This definition was adopted by R. K. Smith, Jr. and M. Danos, in Proceedings of the Topical Conference on Heavy-Ion Collisions, Fall Creek Falls State Park, Pikeville, Tennessee, 1977 [Oak Ridge National Laboratory Report No. CONF-770602, 1977 (unpublished)], p. 363.
[31]W. D. Myers, Lawrence Berkeley Laboratory Report No. LBL-6569, 1977 (unpublished).
[32]W. D. Myers (unpublished).
[33]J. Gosset, J. I. Kapusta, and G. D. Westfall, Lawrence Berkeley Laboratory Report No. LBL-7139, 1978 (unpublished).
[34]J. I. Kapusta (unpublished).
[35]G. D. Westfall, J. Gosset, P. J. Johansen, A. M. Poskanzer, W. G. Meyer, H. H. Gutbrod, A. Sandoval, and R. Stock, Phys. Rev. Lett. 37, 1202 (1976).

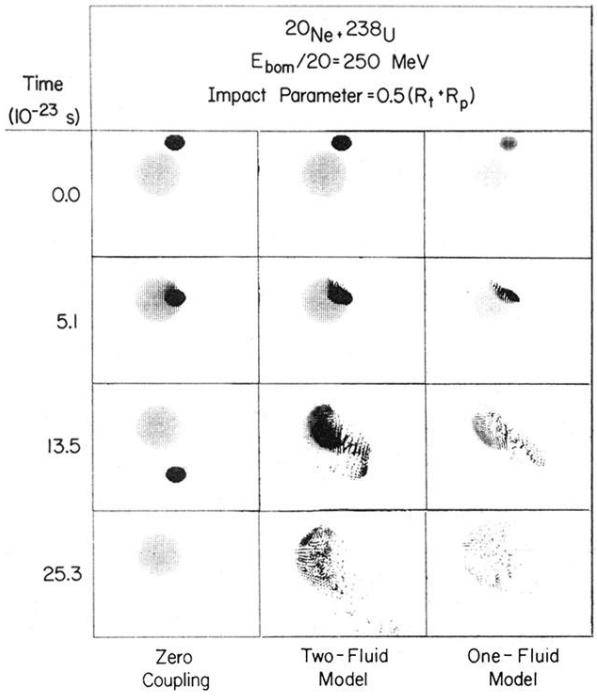

FIG. 1. Calculated time evolution of the matter distribution in the collision of ^{20}Ne with ^{238}U for three different values of the coupling between the two fluids. The left-hand column gives the result for zero coupling, where the target and projectile pass through each other without interaction. The middle column gives the result for a finite coupling taken from free nucleon-nucleon scattering, which corresponds to the present two-fluid model. The right-hand column gives the result for infinite coupling, which corresponds to the previous one-fluid model (Ref. 14). The impact parameter is 0.5 $(R_t + R_p) = 0.5\ (1.2049)(A_t^{1/3} + A_p^{1/3})$ fm, and the laboratory bombarding energy per nucleon is 250 MeV.

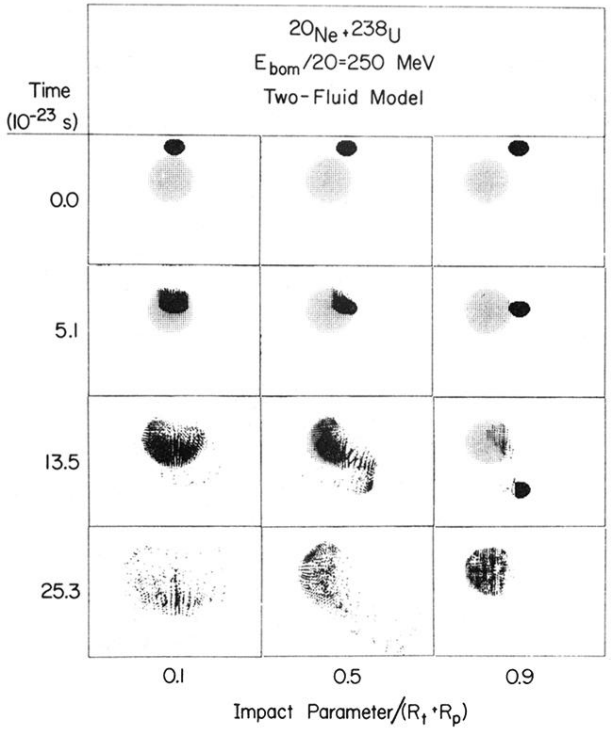

FIG. 2. Calculated time evolution of the matter distribution in the collision of ^{20}Ne with ^{238}U for three different impact parameters. The laboratory bombarding energy per nucleon is 250 MeV.

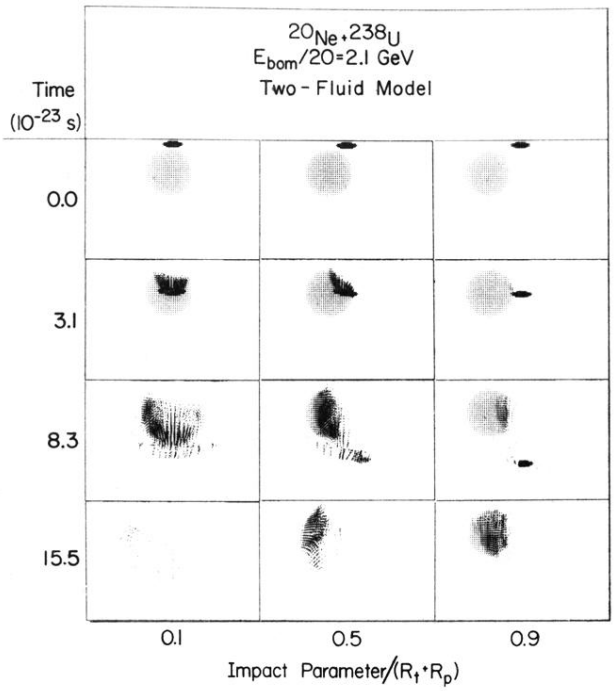

FIG. 3. Calculated time evolution of the matter distribution in the collision of ^{20}Ne with ^{238}U for three different impact parameters. The laboratory bombarding energy per nucleon is 2.1 GeV.